

Shortest Paths for a Robot with Nonholonomic and Field-of-View Constraints

Paolo Salaris*, Daniele Fontanelli†, Lucia Pallottino* and Antonio Bicchi*

Abstract—This paper presents a complete characterization of shortest paths to a goal position for a robot with unicycle kinematics and an on-board camera with limited Field-Of-View (FOV), which must keep a given feature in sight.

Previous work on this subject has shown that the search for a shortest path can be limited to simple families of trajectories. In this paper, we provide a complete optimal synthesis for the problem, i.e. a language of optimal control words, and a global partition of the motion plane induced by shortest paths, such that a word in the optimal language is univocally associated to a region and completely describes the shortest path from any starting point in that region to the goal point. An efficient algorithm to determine the region in which the robot is at any time is also provided.

Index Terms—Nonholonomic Motion Planning; Shortest Path Synthesis; Visual Servoing

I. INTRODUCTION

This paper deals with the study of shortest paths for a directed point moving in a plane to reach a target position while making so that a point fixed in the plane is kept inside a cone moving with the point. The point moves subject to the constraint that its instantaneous velocity is aligned with its direction.

This problem is motivated by several applications in mobile robotics, where a vehicle with nonholonomic kinematics of the unicycle (or Chaplygin sleigh) type, equipped with a limited Field-Of View (FOV) camera, has to reach a target while keeping an environment feature in sight. An inspiring motivation for the study, however, comes from the naturalistic observation of paths followed by raptors during hunting activities [1], see fig. 1. Indeed, the most acute vision information for raptors comes from their deep foveae, which point at approximately 45° to the right or the left of the head axis. The deep fovea system has a limited FOV, so that raptors possess no accurate front sight. This causes a conflict, for instance in falcons, which dive a prey from great distances at high speeds: at a speed of 70 m/s, turning their head sideways to view the prey with high visual acuity may increase aerodynamic drag by a factor of 2 or more, and slow the raptor down. In [1], it has been shown that raptors resolve this conflict by diving along a logarithmic spiral path with their head straight and one eye looking sideways at the prey, rather than following the straight path to the prey with their head turned sideways (see fig. 1).

This paper deals with a closely related problem in robotics, which is the following: given a robot vehicle with an on-board,

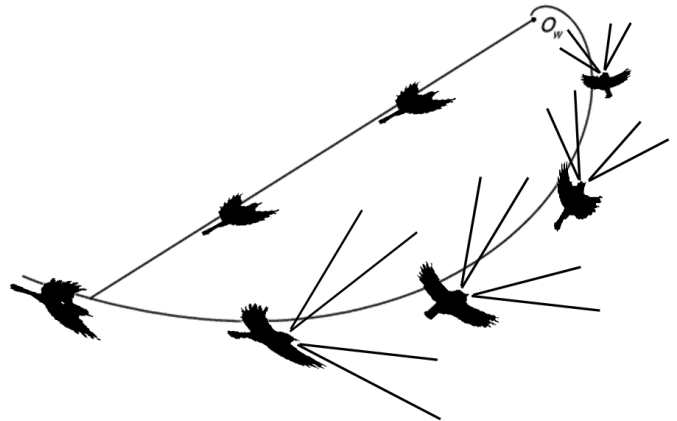


Fig. 1. In order to keep the prey in view, a raptor follows a logarithmic spiral rather than a straight line (cf. [1])

limited FOV camera, and subject to nonholonomic constraints on its motion, find the shortest path to reach a goal, such that a specified feature of the environment is always kept in sight.

The literature of optimal (shortest) paths stems mainly from the seminal work on unicycle vehicles by Dubins [2]. Dubins gave a characterization of shortest curves for a car with a bounded turning radius, proving that optimal solutions consist of combinations of circular arcs of minimum curvature (denoted by the symbols R and L for right and left arcs, respectively) and straight lines (S). He showed that an optimal path can always be found among 6 types only, described by words using at most three such symbols. A complete *optimal control synthesis* for this problem, i.e. a finite partition of the whole motion plane in regions such that the same word encodes the shortest path from all points in the same region, has been reported in [3]. Later on, Reeds and Shepp [4] solved a similar problem with the car moving both forward and backward. This problem was revisited, and the solution refined by the use of tools from optimal control theory, by Sussmann and Tang in [5]. Souères and Laumond in [6] combine necessary conditions given by Pontryagin’s Maximum Principle (PMP) with Lie algebraic tools to provide a global synthesis for the Reeds and Shepp vehicle. The PMP and Lie algebras have been used also to obtain minimum wheel rotation paths in [7] for differential-drive robots. More recently, [8] authors propose an alternative algorithm to determine time optimal trajectories for nonholonomic bidirectional robots using switching vectors. The problem of time optimal trajectories has also attracted considerable attention, as e.g. related to differential-drive robots, for which a complete solution was given by [9].

The optimal control of visually guided robotic manipulators has also received considerable attention recently (see

This work was supported by E.C. under Contract IST 224428 (2008) “CHAT”

* The Interdept. Research Center “Enrico Piaggio”, University of Pisa, via Diotisalvi 2, 56100 Pisa, Italy. paolo.salaris, l.pallottino, bicchi@ing.unipi.it

†Department of Engineering and Information Science, University of Trento, Via Sommarive 14, 38050 Trento (TN), Italy. Phone: +390461883967. Fax: +390461882093. fontanelli@disi.unitn.it

e.g. [10]). Optimal trajectory planning for robot manipulators controlled via a limited FOV camera has been first presented in [11], where two algorithms based on homography and on epipolar geometry, respectively, have been proposed to generate the optimal trajectory of the robot to its goal configuration. Minimal trajectories have been also presented in [12] in case of large displacements, again for a six degrees of freedom robot manipulator. To date, much less is the work that has been devoted to optimal control of visually-servoed robotic vehicles. To the best of the authors' knowledge, the work in [13] and [14] represent the first attempts to find minimum length paths for nonholonomic vehicles equipped with limited FOV monocular cameras.

In this paper, we start from the observation made in [13] that extremal arcs for the considered problem are of three types: rotations on the spot (which will be denoted by the symbol $*$), straight lines (S) and left and right logarithmic spirals (T^L and T^R). The optimal control synthesis presented in [13] consists of 10 regions, for each point of which the shortest path is of the same type and described by a word using up to 3 symbols. In this paper we study the same problem, and show that the synthesis of [13] is valid locally, i.e. for starting positions of the robot close enough to the goal. However, a correct and complete synthesis for the whole plane of motion requires a finer partition in 18 regions, and the use of words of up to 5 symbols. Moreover, an efficient algorithm to determine the region in which the robot is at any time is provided showing that the region can be determined verifying at most 6 elementary inequalities on the initial position.

The approach that we use is based on the exploitation of geometric symmetries and invariants (section III). A synthesis is obtained first for the points on the border of a compact subset of the motion space (section IV), then for the interior of this subset (section V), and finally extended to the entire motion plane (section VI).

II. PROBLEM DEFINITION

Consider a vehicle moving on a plane where a right-handed reference frame $\langle W \rangle$ is defined with origin in O_W and axes X_W, Z_W . The configuration of the vehicle is described by $\xi(t) = (x(t), z(t), \theta(t))$, where $(x(t), z(t))$ is the position in $\langle W \rangle$ of a reference point in the vehicle, and $\theta(t)$ is the vehicle heading with respect to the X_W axis (see fig. 2). We assume that the dynamics of the vehicle are negligible, and that the forward and angular velocities, $v(t)$ and $\omega(t)$ respectively, are the control inputs to the kinematic model of the vehicle. Choosing polar coordinates for the vehicle (see fig. 2), i.e. setting

$$\eta = \begin{bmatrix} \rho \\ \psi \\ \beta \end{bmatrix} = \begin{bmatrix} \sqrt{x^2 + z^2} \\ \arctan\left(\frac{z}{x}\right) \\ \arctan\left(\frac{z}{x}\right) - \theta + \pi \end{bmatrix}, \quad (1)$$

the kinematic model of the unicycle-like robot is

$$\begin{bmatrix} \dot{\rho} \\ \dot{\psi} \\ \dot{\beta} \end{bmatrix} = \begin{bmatrix} -\cos\beta & 0 \\ \frac{\sin\beta}{\rho} & 0 \\ \frac{\sin\beta}{\rho} & -1 \end{bmatrix} \begin{bmatrix} v \\ \omega \end{bmatrix}. \quad (2)$$

We consider vehicles with bounded velocities which can turn on the spot. In other words, we assume

$$(v, \omega) \in U, \quad (3)$$

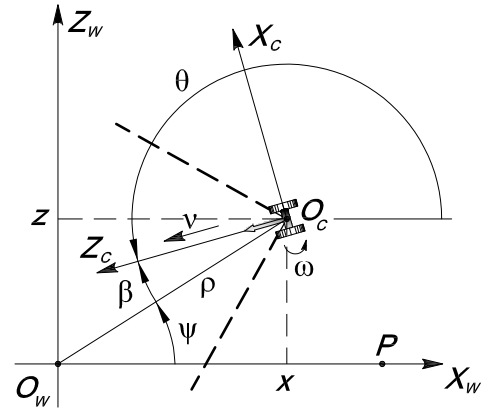


Fig. 2. Mobile robot and systems coordinates. The robot's task is to reach P while keeping O_W within a limited FOV (dashed lines).

with U a compact and convex subset of \mathbb{R}^2 , containing the origin in its interior.

The vehicle is equipped with a rigidly fixed pinhole camera with a reference frame $\langle C \rangle = \{O_C, X_C, Y_C, Z_C\}$ such that the optical center O_C corresponds to the robot's center $[x(t), z(t)]^T$ and the optical axis Z_C is aligned with the robot's forward direction.

Without loss of generality, we consider the position of the robot target point P to lay on the X_W axis, with coordinates $(\rho, \psi) = (\rho_P, 0)$. We also assume that the feature to be kept within the on-board camera FOV is placed on the axis through the origin O_W and perpendicular to the plane of motion. We consider a symmetric planar FOV with characteristic angle $\delta = 2\phi$, which generates the constraints

$$\beta + \phi \geq 0, \quad (4)$$

$$\beta - \phi \leq 0. \quad (5)$$

Noticed that we place no restrictions on the vertical dimension of the FOV. Therefore, the height of the feature on the motion plane, which corresponds to its Y_C coordinate in the camera frame $\langle C \rangle$, is irrelevant to our problem. Hence, for our purposes, it is necessary to know only the projection of the feature on the motion plane, i.e. O_W .

The goal of this paper is to determine, for any point $Q \in \mathbb{R}^2$ in the robot space, the shortest path from Q to P such that the feature is maintained in the camera field of view. In other words, we want to minimize the length of the path covered by the center of the vehicle, i.e. to minimize the cost functional

$$L = \int_0^\tau |v| dt,$$

under the *feasibility constraints* (2), (3), (4), and (5). Here, τ is the time needed to reach P that is $\rho(\tau) = \rho_P, \psi(\tau) = 0$.

The time derivative of the FOV constraints computed along the trajectories of system (2) brings to

$$\dot{\beta} = \frac{\sin\beta}{\rho} v - \omega, \quad (6)$$

for both constraints. From the theory of optimal control, with state and control constraints [15], the associated Hamiltonian

is

$$H(\eta, \nu, \omega) = |\nu| - \lambda_1 \cos \beta \nu + \lambda_2 \frac{\sin \beta}{\rho} \nu + (\lambda_3 + \mu_1 + \mu_2) \left(\frac{\sin \beta}{\rho} \nu - \omega \right),$$

with $\lambda = (\lambda_1, \lambda_2, \lambda_3) \neq 0$ and $\mu = (\mu_1, \mu_2) \geq 0$. When the FOV constraints are not active (i.e. $\mu = 0$), extremal curves (i.e. curves that satisfy necessary conditions for optimality) include straight lines (corresponding to $\omega = 0$ and denoted by the symbol S) and rotations on the spot (corresponding to $\nu = 0$ and denoted by the symbol $*$).

On the other hand, when $\mu > 0$ we have

$$\begin{aligned} \beta + \phi \equiv 0 &\Rightarrow \tan \beta = -\tan \phi \\ \beta - \phi \equiv 0 &\Rightarrow \tan \beta = \tan \phi, \end{aligned}$$

and, by (2),

$$\dot{\psi} = \tan \phi \frac{\dot{\rho}}{\rho} = \tan \phi \frac{d}{dt} (\ln \rho), \text{ when } \beta = -\phi \quad (7)$$

$$\dot{\psi} = -\tan \phi \frac{\dot{\rho}}{\rho} = -\tan \phi \frac{d}{dt} (\ln \rho), \text{ when } \beta = \phi. \quad (8)$$

By integration, we obtain

$$\psi = \tan \phi \ln \left(\frac{\rho}{\rho_o} \right), \text{ when } \beta = -\phi \quad (9)$$

$$\psi = -\tan \phi \ln \left(\frac{\rho}{\rho_o} \right), \text{ when } \beta = \phi \quad (10)$$

where ρ_o is a constant that depends on initial conditions.

Equations (9) and (10) represent two logarithmic spirals rotating counterclockwise and clockwise around the feature, respectively. We refer to these two spirals as *Right* and *Left*, and by symbols T^R and T^L , respectively. The adjectives “right” and “left” indicate the half-plane where the spiral starts for an on-board observer aiming at the feature.

We have thus obtained four extremal maneuvers, represented by the symbols $\{*, S, T^R, T^L\}$. Rotations on the spot ($*$) have zero length, but may be used to properly connect other maneuvers.

Extremal arcs can be executed by the vehicle in either forward or backward direction: we will hence use superscripts $+$ and $-$ to make this explicit (e.g., S^- stands for a straight line executed backward). In conclusion, we will build extremal paths consisting of sequences, or *words*, comprised of symbols in the alphabet $\{*, S^+, S^-, T^{R+}, T^{R-}, T^{L+}, T^{L-}\}$. The set of possible words generated by the above symbols is a language \mathcal{L} .

The rest of the paper is dedicated to showing that, due to the physical and geometrical constraints of the considered problem, a sufficient optimal finite language $\mathcal{L}_O \subset \mathcal{L}$ can be built such that, for any initial condition, it contains a word describing a path to the goal which is no longer than any other feasible path. Correspondingly, a partition of the plane in a finite number of regions is described, for which the shortest path is one of the words in \mathcal{L}_O .

Notice that, for $\phi \geq \frac{\pi}{2}$, a straight line followed forward and/or backward so as to keep the feature in view is always feasible and, hence, trivially optimal. In the rest of the paper, we will only be concerned with the non-trivial case $\phi \in [0, \frac{\pi}{2}]$.

III. SHORTEST PATHS SYNTHESIS: SYMMETRIES AND INVARIANTS

In this section, we introduce the basic tools that will allow us to study the optimal synthesis on the whole state space of the robot.

Let $\eta(\tau)$ denote a trajectory of the vehicle corresponding to a solution of equations 2 and 3. Because we are interested in finding shortest paths for the vehicle’s center point, we define a *path* γ as the canonical projection of the graph $(\eta(\tau), \tau)$ on the first two coordinates. In other terms, a path γ parameterized by t , is a continuous map from the interval $I = [0, 1]$ to the plane of motion $\gamma(t) = (\rho(t), \psi(t))$, $t \in I$. We denote with \mathcal{P}_Q the set of all feasible extremal paths from $\gamma(0) = Q$ to $\gamma(1) = P$.

Definition 1. Given the target point P , with $P = (\rho_P, 0)$ in polar coordinates, and $Q \in \mathbb{R}^2 \setminus O_W$, $Q = (\rho_Q, \psi_Q)$ with $\rho_Q \neq 0$, let $f_Q: \mathbb{R}^2 \rightarrow \mathbb{R}^2$ denote the map

$$f_Q(\rho_G, \psi_G) = \begin{cases} \left(\frac{\rho_G \rho_P}{\rho_Q}, \psi_Q - \psi_G \right) & \text{for } \rho_G \neq 0 \\ (0, 0) & \text{otherwise.} \end{cases} \quad (11)$$

Remark 1. The map f_Q can be regarded as the combination of a clockwise rotation R_Q by an angle ψ_Q , a scaling S_Q by a factor ρ_P/ρ_Q , and an axial symmetry w.r.t. X_W . Indeed, if $R_Q: (\rho, \psi) \mapsto (\rho, \psi - \psi_Q)$ and $S_Q: (\rho, \psi) \mapsto (\rho(\rho_P/\rho_Q), \psi)$, we have $R_Q \circ S_Q: (\rho, \psi) \mapsto (\rho \rho_P/\rho_Q, \psi - \psi_Q)$.

Definition 2. Given the target point $P = (\rho_P, 0)$ and $Q = (\rho_Q, \psi_Q)$ with $\rho_Q \neq 0$, let the path transform function F_Q be defined as

$$\begin{aligned} F_Q: \mathcal{P}_Q &\rightarrow \mathcal{P}_{f_Q(P)} \\ \gamma(t) &\mapsto f_Q(\gamma(1-t)), \forall t \in I. \end{aligned} \quad (12)$$

Remark 2. Notice that $\tilde{\gamma}(t) = F_Q(\gamma(1-t))$ corresponds to $\gamma(t)$ transformed by f_Q and followed in opposite direction. Indeed, $\tilde{\gamma}$ is a path from $\tilde{\gamma}(0) = f_Q(P)$ to $\tilde{\gamma}(1) = f_Q(Q) \equiv P$.

Turning our attention back to the map $f_Q(\cdot)$, it can be noticed that point Q is transformed in $f_Q(Q) = P$, while P goes into $f_Q(P) = \left(\frac{\rho_P^2}{\rho_Q}, \psi_Q \right)$.

Consider now the locus of points Q such that it further holds $f_Q(P) = Q$. This is clearly the circumference with center in O_W and radius ρ_P . We will denote this circumference, which will have an important role in the following developments, by $C(P)$. Properties of F_Q will allow us to solve the synthesis problem from points on $C(P)$, hence to extend the synthesis to any point inside the circle, and finally to the whole motion plane.

Remark 3. As a first consequence of the fact that $\forall Q \in C(P)$, $f_Q(P) = Q$ and $f_Q(Q) = P$, we have that \mathcal{P}_Q is F_Q -invariant, i.e. $Q \in C(P) \Rightarrow \forall \gamma \in \mathcal{P}_Q, F_Q(\gamma) \in \mathcal{P}_{f_Q(P)} \equiv \mathcal{P}_Q$.

Notice that Remark 1 is valid also for F_Q . As a consequence $F_{f_Q(P)}(F_Q(\gamma)) \equiv \gamma$. Furthermore, F_Q transforms forward straight lines in backward straight lines and viceversa. Moreover, F_Q maps left spiral arcs (T^{L+} and T^{L-}) in right spiral arcs (T^{R-} and T^{R+} respectively) and viceversa. Hence, F_Q maps extremal paths in \mathcal{L} in extremal paths in \mathcal{L} . For example, let $w = S^- * T^{R-} * S^+ * T^{L+}$ be the word that characterize a

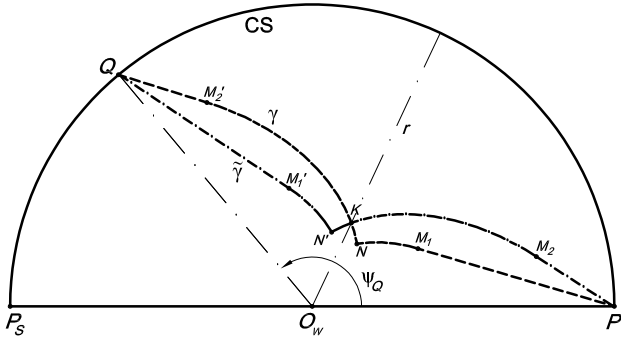


Fig. 3. Construction of a palindrome symmetric path: γ is a generic path from Q to P and $\tilde{\gamma}$ the symmetric to γ w.r.t. the bisectrix r .

path from Q to P , the transformed extremal path is of type $z = T^{R-} * S^- * T^{L+} * S^+$. With a slight abuse of notation, we will write $z = F_Q(w)$.

From previous remarks we also obtain that an extremal path $\gamma \in \mathcal{P}_Q$ with $Q \in C(P)$ is mapped in an extremal path $\tilde{\gamma} \in \mathcal{P}_Q$ symmetric to γ w.r.t. the bisectrix r of the angle $\widehat{QO_w P}$.

In the following, we will denote by $D(P)$ the closed disc within $C(P)$. Due to the symmetry of the problem, however, the analysis of optimal paths in \mathcal{P}_Q can be done considering only the upper half plane w.r.t. the X_w axis. We denote therefore by DS the closure of the semidisk in the positive Z_w half-plane, by CS the upper semicircumference, and by $\widehat{P_s P}$ the diameter such that $\partial DS = CS \cup \widehat{P_s P}$ (see fig. 3).

Proposition 1. *Given $Q \in \mathbb{R}^2$ and a path $\gamma \in \mathcal{P}_Q$ of length l , the length of the transformed path $\tilde{\gamma} = F_Q(\gamma)$ is $\tilde{l} = \frac{\rho_P}{\rho_Q} l$.*

Proof: Given $Q \in (X_w, Z_w)$, from Remark 1, straight lines are scaled by ρ_P/ρ_Q . The distance of two points $P_1 = (\rho_1, \psi_1)$ and $P_2 = (\rho_2, \psi_2)$ on a logarithmic spiral with characteristic angle ϕ is $d = (\rho_1 - \rho_2)/\cos \phi$. Hence, the distance between transformed points is scaled by ρ_P/ρ_Q . The total path length is thus scaled by ρ_P/ρ_Q , i.e. increased if $Q \in DS$ and decreased if $Q \notin DS$. ■

Definition 3. *An extremal path starting from Q and described by a word $w \in \mathcal{L}$ is a palindrome path if the transformed path through F_Q is also described by w .*

Definition 4. *An extremal path in \mathcal{P}_Q which is a palindrome path and is symmetric w.r.t. the bisectrix r of $\widehat{QO_w P}$, is called a palindrome symmetric path.*

Proposition 2. *For any path in \mathcal{P}_Q with $Q \in CS$ there always exists a palindrome symmetric path in \mathcal{P}_Q whose length is shorter or equal.*

Proof: Consider $\gamma \in \mathcal{P}_Q$ with $Q \in CS$, and $\tilde{\gamma} = F_Q(\gamma)$ the transformed path, which is symmetric to γ w.r.t. the bisectrix r of $\widehat{QO_w P}$ (see fig. 3). Indeed, in this case, F_Q consists only in a rotation and axial symmetry, hence it corresponds to the bisectrix symmetry. Hence, from Proposition 1, γ and $\tilde{\gamma}$ have the same length l . Let $K \in r$ be the intersection point of the two paths, we denote with γ_1 and γ_2 ($\tilde{\gamma}_1$ and $\tilde{\gamma}_2$) the sub-paths of γ ($\tilde{\gamma}$) from Q to K and from K to P respectively. From the definition of $\tilde{\gamma}$ we have that the length l_1 of γ_1 is equal to the length \tilde{l}_2 of $\tilde{\gamma}_2$, and the length l_2 of γ_2 is equal to the length \tilde{l}_1 of $\tilde{\gamma}_1$. Furthermore, $l_1 + l_2 = \tilde{l}_1 + \tilde{l}_2 = l$.

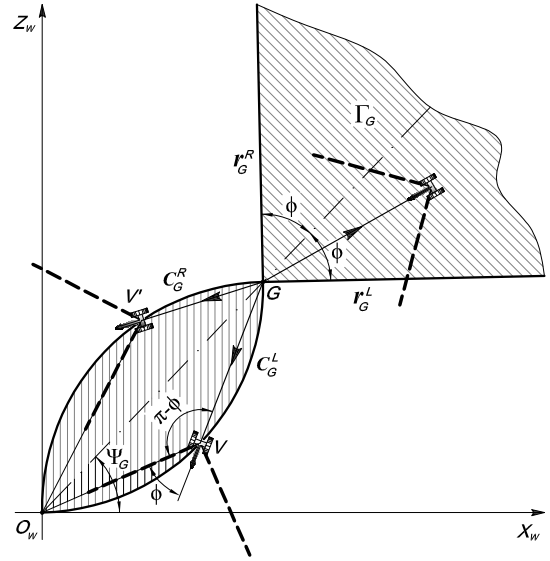


Fig. 4. Region C_G with its border $\partial C_G = C_G^R \cup C_G^L$ and cone Γ_G delimited by half-lines r_G^R and r_G^L .

Suppose that $l_1 \geq l_2 = \tilde{l}_1$, then the path from Q to P obtained from a concatenation of $\tilde{\gamma}_1$ and γ_2 has length $\tilde{l}_1 + l_2 = 2l_2$ smaller than, or equal to, the length l of γ , and it is feasible and symmetric w.r.t. the bisectrix r , i.e. a palindrome symmetric path. If $l_1 < l_2$ the construction of a palindrome symmetric path can be done equivalently using γ_1 and $\tilde{\gamma}_2$. ■

An important consequence of the properties of the path transform F_Q is the following

Theorem 1. *For any path in \mathcal{P}_Q with $Q \in \partial DS$ there always exists a path in \mathcal{P}_Q which evolves completely within DS whose length is shorter or equal.*

Proof: We first prove that for any path δ between two points in $C(P)$, there exists a path completely inside $D(P)$ whose length is shorter or equal. Let Q' and P' be the extremal points of a sub-path of δ completely outside $D(P)$, and let l be length of such sub-path. From Proposition 2, there exists a palindrome path γ from Q' to P' of length l or shorter that evolves completely outside $D(P)$. The intersection of γ with the bisectrix r of the angle $\widehat{P'O_w Q'}$ is a point Z , with $\rho_Z > \rho_P$. By symmetry, the length of the sub-path γ_Z from Z to P' is $l/2$. On the other hand, γ_Z is transformed by F_Z in $\tilde{\gamma}_Z$, going from $F_Z(Z)$ to P' , with length $\frac{\rho_P}{\rho_Z} \frac{l}{2}$. Joining $\tilde{\gamma}_Z$ with its symmetric with respect to r , a path from Q' to P' of length $\frac{\rho_P}{\rho_Z} l < l$ is found.

As a consequence, any path from $Q \in C(P)$ to P can be shortened by an extremal feasible path completely inside $D(P)$. Moreover, for Q on ∂DS , γ evolves in DS : indeed, if there existed a point of intersection \tilde{Z} with the X_w axis, the sub-path $\gamma_{\tilde{Z}}$ from \tilde{Z} to P would be shortened by the segment $\tilde{Z}P$ lying on the axis itself, i.e. on $\widehat{P_s P}$. ■

IV. OPTIMAL PATHS FOR POINTS ON CS

Our study of the optimal synthesis begins in this section addressing optimal paths from points on CS. We preliminarily establish an existence result.

Proposition 3. For any $Q \in CS$ there exists a feasible shortest path to P .

Proof: Because of state constraints (4), and (5), and the restriction of optimal paths in DS (Theorem 1) the state set is compact. Furthermore, for any point at distance ρ from O_W the optimal path is shorter or equal to $\rho + \rho_P$ (which corresponds to the path $S^+ * S^-$ through O_W). The system is also controllable (cf. [13]). Hence, Filippov existence theorem for Lagrange problems can be invoked [16]. ■

A first simple result can be stated for starting points on the diameter $\overline{P_S P}$ of $C(P)$.

Proposition 4. For $Q \in \overline{P_S O_W}$ the optimal path is $S^+ * S^-$ with switching point in O_W . For $Q \in \overline{O_W P}$ the optimal path is S^- .

Proof: The FOV constraint is not active from Q to O_W and from O_W to P , hence a straight line is the shortest path. ■

Definition 5. For a point $G \in \mathbb{R}^2$, let C_G^R (C_G^L) denote the circular arc from G to O_W such that, $\forall V \in C_G^R$ (C_G^L), $\widehat{GVO_W} = \pi - \phi$ in the half-plane on the right (left) of $\overline{GO_W}$ (cf. fig. 4). Also, let C_G denote the region delimited by C_G^R and C_G^L from G to O_W .

We will refer to C_G^R (C_G^L) as the right (left) ϕ -arc in G .

Definition 6. For a point $G \in \mathbb{R}^2$, let r_G^R (r_G^L) denote the half-line from G forming an angle $\psi_G + \phi$ ($\psi_G - \phi$) with the X_W axis (cf. fig. 4). Also, let Γ_G denote the cone delimited by r_G^R and r_G^L .

We will refer to r_G^R (r_G^L) as the right (left) ϕ -radius in G . The following result is obtained by elementary geometric arguments:

Proposition 5. For any starting point Q , all points of C_Q are reachable by a straight path without violating the FOV constraint.

A sufficient family of (palindrome symmetric) optimal paths is obtained in the following theorem.

Theorem 2. For any $Q \in CS$ to P there exists a palindrome symmetric shortest path of type $S^+ T^{L+} * T^{R-} S^-$.

To prove Theorem 2, we establish first a few preliminary results.

Proposition 6. If an optimal path $\gamma \in \mathcal{P}_Q$ includes a segment of type S^+ with extremes in A, B , then either $B = P \in C_A$ or $B \in C_A^R \cup C_A^L$.

Proof: If $B \notin C_A$ the straight line violates either one of the FOV constraints. Furthermore, if $B \in C_A$ but $B \notin \partial C_A$ and $P \notin C_A$, the sub-path from B to P intersects ∂C_A in B' . Hence, γ could be shortened by replacing the sub-path from A to B' through B with the segment $\overline{AB'}$. If $P \in C_A$, then by the optimality principle $B = P$. ■

Remark 4. The argument of Proposition 6 can be repeated for any point A' on the S^+ segment ending in B . Hence, for any forward segment \overline{AB} of an optimal path $\gamma \in \mathcal{P}_Q$, it holds either $B \in \bigcap_{A' \in \overline{AB}} \partial C_{A'}^R$ or $B \in \bigcap_{A' \in \overline{AB}} \partial C_{A'}^L$. Notice that this holds also for the particular cases $B = P$ and $B = O_W$.

Proposition 7. If an optimal path $\gamma \in \mathcal{P}_Q$ includes a segment of type S^- with extremes in B, A , then either $A = P \in \Gamma_B$ or $A \in r_B^R \cup r_B^L$.

Proof: If $A \notin \Gamma_B$ the straight line violates either one of the FOV constraints. Furthermore, if $A \in \Gamma_B$ but $A \notin \partial \Gamma_B$ and $P \notin \Gamma_B$, the sub-path from A to P intersects $\partial \Gamma_B$ in A' . Hence, γ could be shortened by replacing the sub-path from B to A' through A with the segment $\overline{BA'}$. If $P \in \Gamma_B$, then by the optimality principle $A = P$. ■

Proposition 8. If a path $\gamma(t)$, $t \in [0, 1]$ is optimal, then its angle $\psi(t)$ is monotonic.

Proof: Because γ is a continuous path, the angle of its points varies continuously. Should the angle be not monotonic (i.e. neither monotonically non-decreasing nor monotonically non-increasing), then there would exist two points on the path with the same angle, hence aligned with O_W . These two points could be connected with a feasible straight line, thus shortening γ , which on the contrary was supposed to be a shortest path. ■

Remark 5. By applying Proposition 8 to optimal paths from Q in the upper half-plane to P , and noticing that $\psi_Q \geq \psi_P = 0$, the angle is non increasing. Hence optimal paths in the upper half-plane, and in particular in DS , do not include counter-clockwise extremals of type T^{R+} or T^{L-} .

Proposition 9. If a path $\gamma(t)$ is optimal, then its distance $\rho(t)$ has no local maximum for $t \in (0, 1)$.

Proof: Because γ is a continuous path, the distance $\rho(t)$ of its points from O_W is a continuous function of t . Assume that the distance has a maximum in an internal point $\bar{t} \in (0, 1)$. Then, by classical analysis theorems, there exist two values t_G and t_H in $(0, 1)$ such that $\rho(t_G) = \rho(t_H) < \rho(\bar{t})$, with the sub-path between t_G and t_H evolving outside the disk of radius $\rho(t_G)$. Applying the same arguments used in the proof of Theorem 1, replacing Q' with $\gamma(t_G)$ and P' with $\gamma(t_H)$, it is shown that a shorter sub-path between t_G and t_H exists evolving completely within the disk, i.e. a contradiction. ■

Remark 6. Observe that the distance from O_W is strictly increasing along backward extremal arcs (i.e. S^- , T^{R-} , T^{L-}) and strictly decreasing along forward extremal arcs (i.e. S^+ , T^{R+} , T^{L+}). As a consequence of Proposition 9 in an optimal path a forward arc cannot follow a backward arc.

Proposition 10. For any two points G, H , consider a spiral arc T (either left or right) from G to H , and denote by r_G, r_H the tangent lines to T in G and H , respectively. Let $A = r_G \cap r_H$. Then, the length of T is less than the sum of lengths of the segments \overline{GA} and \overline{AH} (see fig. 5).

Proof: We prove this statement by building a sequence of piecewise linear paths shorter than $\overline{GA} \cup \overline{AH}$ which approximates the arc T . Let B be the intersection point with T of the line from O_W to A (see fig. 5). The line r_B tangent to T in B intersects \overline{GA} and \overline{AH} in C and D , respectively. The path $\overline{GC} \cup \overline{CD} \cup \overline{DH}$ is shorter than $\overline{GA} \cup \overline{AH}$. The same construction and reasoning can be applied now to the sub-arcs of T from G to B , and from B to H , and so on. Inductively, the logarithmic spiral between G to H is asymptotically approximated by a sequence of piecewise unfeasible paths shorter than $\overline{GA} \cup \overline{AH}$,

hence the thesis. ■

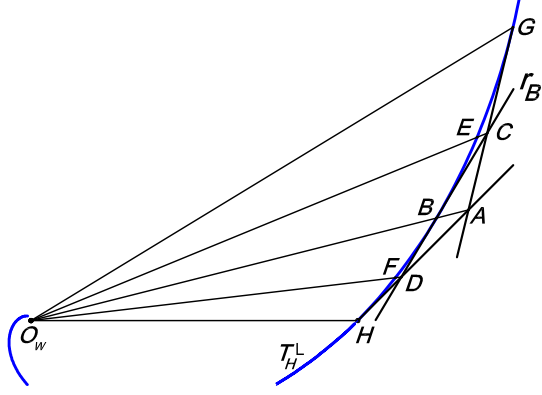


Fig. 5. Construction used in the proof of Proposition 10.

Proposition 11. Any path of type $S^- * T^{R-}$ (resp., $T^{L+} * S^+$) can be shortened by a path of type $T^{R-} S^-$ (resp., $S^+ T^{L+}$).

Proof: Let A and B be the initial and final points of the $S^- * T^{R-}$, and let A_1 be the switching point between S^- and T^{R-} (see fig. 6). Without loss of generality, we assume that A_1 belongs to r_A^L , the left ϕ -radius in A (if not, the path can be shortened by a path of the same type for which this is true). Let G be the intersection point between the spiral T_A^R through A and the ϕ -arc C_B^R through B . By Definitions 5,6, and the properties of logarithmic spirals, the line r_G through B and G is tangent to T_A^R in G , while r_A^L is tangent to T_A^R in A . Let A' be the intersection of r_G with r_A^L . The segment $A'B$ is shorter than the sub-path $S^- * T^{R-}$ from A' to B through A_1 . By Proposition 10, however, the feasible spiral arc T_A^R from A to G shortens $AA' \cup A'G$, hence the thesis. The proof for $T^{L+} S^+$ is analogous. ■

Proof of Theorem 2.: According to Propositions 8–11 and Remarks 5–6, a sufficient optimal language \mathcal{L}_O for $Q \in DS$ is described in fig. 7. It is straightforward to observe that the number of switches between extremals is finite and less or equal to 3, and a sufficient family of optimal paths is given by the word $S^+ T^{L+} * T^{R-} S^-$ and its degenerate cases. Furthermore, by Proposition 2, for $Q \in CS$ optimal paths are palindrome symmetric. ■

A palindrome symmetric path from Q on CS to P of the type $S^+ T^{L+} * T^{R-} S^-$ is shown in fig. 8. By symmetry, it follows that the sub-paths S^+ and S^- have the same length, and so do T^{L+} and T^{R-} . As a consequence, only two sub-words $T^{L+} * T^{R-}$ and $S^+ * S^-$ need be considered, which are obtained as degenerate cases with zero length arcs.

Referring to fig. 8, let the switching points of the optimal path be denoted as M_2, N , and M_1 , respectively. Notice that N is on the bisectrix r of \widehat{QOP} , while M_1 and M_2 are symmetric w.r.t. r . In fig. 8 the region C_Q , locus of points reachable by a linear feasible path from Q , is also reported delimited by dashed curves.

We now study the length of extremal paths from CS to P in the sufficient family above. To do so, it is instrumental to parameterize the family by the angular position of the first switching point, α_{M_1} .

Theorem 3. The length of a path $\gamma \in \mathcal{P}_Q$, $Q \in CS$, of type

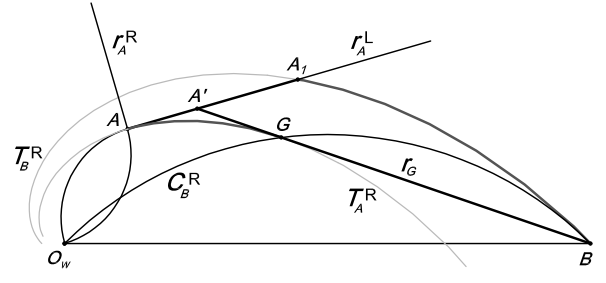


Fig. 6. Construction used in the proof of Proposition 11.

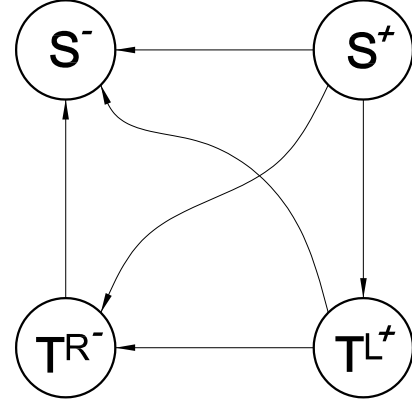


Fig. 7. Feasible extremals and sequences of extremals from points in DS .

$S^+ T^{L+} * T^{R-} S^-$ passing through $M_1 = (\rho_{M_1}, \alpha_{M_1})$ is

$$L = 2 \frac{\rho_P}{\cos \phi} \cos \alpha_{M_1} - \frac{2\rho_P e^{(\alpha_{M_1} - \frac{\psi_Q}{2})t}}{\cos \phi \sin \phi} \sin(\phi - \alpha_{M_1}), \quad (13)$$

when $\phi \in]0, \frac{\pi}{2}[$. In the extreme cases $\phi = 0$ and $\phi = \frac{\pi}{2}$, we have $L = 2\rho_P$ and $L = 2\rho_P \sin \frac{\psi_Q}{2}$, respectively.

Proof: Recalling that $P = (\rho_P, 0)$, $Q = (\rho_P, \psi_Q)$, when $\phi > 0$, $M_1 \in C_P^R$, by the law of sines we have

$$\rho_{M_1} = \rho_P \frac{\sin(\phi - \alpha_{M_1})}{\sin \phi}, \quad (14)$$

On the other hand, for $M_2 = (\rho_{M_2}, \psi_Q - \alpha_{M_2})$ on C_Q^L it holds by symmetry $\rho_{M_2} = \rho_{M_1}$.

Also the lengths of segments S^+ and S^- are equal, and evaluate to

$$\overline{PM_1} = \overline{QM_2} = \rho_P \frac{\sin \alpha_{M_1}}{\sin \phi}. \quad (15)$$

From (9), setting $t = \frac{\cos \phi}{\sin \phi}$, the right logarithmic spiral passing through M_1 (denoted with $T_{M_1}^R$) is given by

$$T_{M_1}^R : \left(\rho_{M_1} e^{(\alpha_{M_1} - \psi)t}, \psi \right).$$

Similarly, the left spiral for M_2 (denoted with $T_{M_2}^L$) is given by

$$T_{M_2}^L : \left(\rho_{M_2} e^{-(\psi_Q - \alpha_{M_2} - \psi)t}, \psi \right).$$

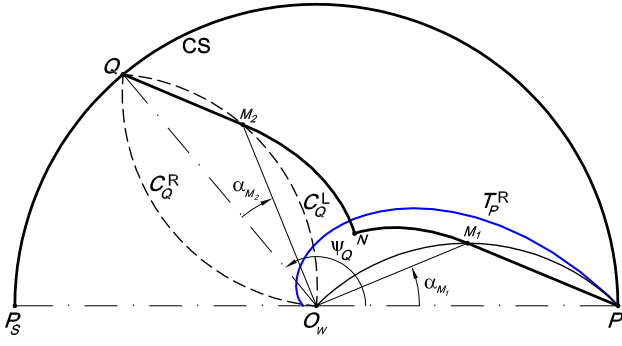


Fig. 8. The palindrome symmetric path of type $S^+ T^{L+} * T^{R-} S^-$ from $Q \in CS$ to P .

The intersection point between the spirals $T_{M_1}^R$ and $T_{M_2}^L$ is $N = (\rho_N, \psi_N)$, where

$$\begin{aligned} \rho_N &= \rho_P \frac{e^{\frac{(\alpha_{M_1} - \psi_Q + \alpha_{M_2})t}{2}}}{\sin \phi} \sqrt{\sin(\phi - \alpha_{M_1}) \sin(\phi - \alpha_{M_2})} = \\ &= \rho_P \frac{e^{\frac{(\alpha_{M_1} - \psi_Q)t}{2}}}{\sin \phi} \sin(\phi - \alpha_{M_1}) \end{aligned} \quad (16)$$

$$\psi_N = \frac{(\alpha_{M_1} + \psi_Q - \alpha_{M_2})}{2} - \frac{\cos \phi}{2 \sin \phi} \ln \left(\frac{\sin(\phi - \alpha_{M_2})}{\sin(\phi - \alpha_{M_1})} \right) = \frac{\psi_Q}{2}. \quad (17)$$

Notice that for $\phi = \frac{\pi}{2}$ we have $M_1 \equiv M_2 \equiv N$ and spiral arcs have zero length. Hence, from (15) and (17), $L = 2\rho_P \sin \frac{\psi_Q}{2}$.

For $\phi \in]0, \frac{\pi}{2}[$, the length of the spiral arcs T^{L+} from M_1 to N and T^{L-} from M_2 to N are equal, and evaluate to

$$\overline{M_1 N} = \overline{M_2 N} = \frac{\rho_{M_1} - \rho_N}{\cos \phi}.$$

Adding up, after some simplifications, the total length L is therefore as reported in (13).

When $\phi = 0$, $M_1 \equiv M_2 \equiv O_w$ and spiral arcs have zero length, hence $L = 2\rho_P$. ■

Having an analytical expression for the length of the path as a function of a single parameter α_{M_1} (hence indirectly of $Q \in CS$), we are now in a position to minimize the length within the sufficient family. Notice that we need only to consider $\alpha_{M_1} \geq 0$ (because the problem is symmetric w.r.t. X_w), and $\alpha_{M_1} \leq \phi$ for the geometrical considerations above on C_Q^L (see fig. 4).

Theorem 4. Given $Q = (\rho_P, \psi_Q) \in CS$,

- for $0 < \psi_Q \leq \psi_M \triangleq -4 \tan \phi \ln(\sin \phi)$, the optimal path is of type $T^{L+} * T^{R-}$;
- for $\psi_M < \psi_Q < \psi_V \triangleq 2\phi + \psi_M$, the optimal path is of type $S^+ T^{L+} * T^{R-} S^-$;
- for $\psi_V \leq \psi_Q < \pi$, the optimal path is of type $S^+ * S^-$

Proof: To find the value of $\alpha_{M_1} \in [0, \phi]$ which minimizes the length L , consider the first derivative

$$\frac{\partial L}{\partial \alpha_{M_1}} = 2\rho_P \frac{\sin \alpha_{M_1}}{\cos \phi} \left(\frac{e^{(\alpha_{M_1} - \frac{\psi_Q}{2})t}}{\sin^2 \phi} - 1 \right). \quad (18)$$

The critical points of α_{M_1} are

$${}^a \alpha_{M_1} = 0 \quad (19)$$

$${}^b \alpha_{M_1} = \frac{\psi_Q}{2} + 2 \tan \phi \ln(\sin \phi). \quad (20)$$

To determine the local maximum or minimum nature of the critical values, consider the second derivative of L ,

$$\begin{aligned} \frac{\partial^2 L}{\partial \alpha_{M_1}^2} &= \frac{2\rho_P}{\cos \phi} \left[\cos \alpha_{M_1} \left(\frac{e^{(\alpha_{M_1} - \frac{\psi_Q}{2})t}}{\sin^2 \phi} - 1 \right) + \right. \\ &\quad \left. + \sin \alpha_{M_1} \frac{e^{(\alpha_{M_1} - \frac{\psi_Q}{2})t}}{\tan \phi} \right] \end{aligned} \quad (21)$$

and

$$\left. \frac{\partial^2 L}{\partial \alpha_{M_1}^2} \right|_{{}^a \alpha_{M_1}} = \frac{2\rho_P}{\cos \phi} \left(\frac{e^{-\frac{\psi_Q}{2}t}}{\sin^2 \phi} - 1 \right) \quad (22)$$

$$\left. \frac{\partial^2 L}{\partial \alpha_{M_1}^2} \right|_{{}^b \alpha_{M_1}} = 2\rho_P \sin \phi \sin \left(\frac{\psi_Q}{2} + 2 \tan \phi \ln(\sin \phi) \right) \quad (23)$$

Notice that, when the minimum of L is reached in $\alpha_{M_1} = 0$, the path is of type $T^{L+} * T^{R-}$. From equation (22), the critical point $\alpha_{M_1} = 0$ is a minimum of L if $\left. \frac{\partial^2 L}{\partial \alpha_{M_1}^2} \right|_{{}^a \alpha_{M_1}} \geq 0$, that is, if

$$\psi_Q \leq -4 \tan \phi \ln(\sin \phi) \triangleq \psi_M$$

Hence, the shortest path from Q on CS to P is of type $T^{L+} * T^{R-}$ if the polar coordinate of Q are (ρ_P, ψ_Q) with $\psi_Q \in [0, \psi_M]$. The point on CS whose polar coordinates are (ρ_P, ψ_M) is point M .

On the other hand, from equation (23), if $\psi_M < \psi_Q \leq \pi$ the minimum of L is reached in $\alpha_{M_1} \in (0, \phi)$. This critical point depends on ψ_Q , as shown in (20), i.e. $\alpha_{M_1} = \frac{\psi_Q - \psi_M}{2}$. In this case, the shortest path is of type $S^+ T^{L+} * T^{R-} S^-$.

When the minimum of L is reached in $\alpha_{M_1} = \phi$, the optimal path is of type $S^+ * S^-$. The first value $\psi_Q \in (\psi_M, \pi]$ such that the optimal path is reached in $\alpha_{M_1} = \phi$ is, from equation (20),

$$2\phi - 4 \tan \phi \ln(\sin \phi) = 2\phi + \psi_M \triangleq \psi_V.$$

The point on CS whose polar coordinates are (ρ_P, ψ_V) is point V . For all starting points Q between V and P_s , the shortest path is of type $S^+ * S^-$. ■

We are now interested in determining the locus of switching points between extremals in optimal paths.

Proposition 12. For $Q \in CS$ with $0 < \psi_Q \leq \psi_M$, the switching locus is the arc of T_P^R within the extreme points P and $m = (\rho_P \sin^2 \phi, \psi_M/2)$ (included).

Proof: From Theorem 4, the optimal path from $Q \in CS$ to P is of type $T^{L+} * T^{R-}$. Hence, the switching occurs in the intersection of T_Q^L and T_P^R . The point of intersection varies on T_P^R from P (when $\psi_Q = 0$) to $m = (\rho_P \sin^2 \phi, \psi_M/2) = T_M^L \cap T_P^R$ (when $\psi_Q = \psi_M$). ■

Proposition 13. For $Q \in CS$ with $\psi_M < \psi_Q < \psi_V$, the loci of switching points M_1 , N , and M_2 are the right ϕ -arcs C_P^R , C_M^R , and C_M^R with $M = (\rho_P, \psi_M)$, respectively.

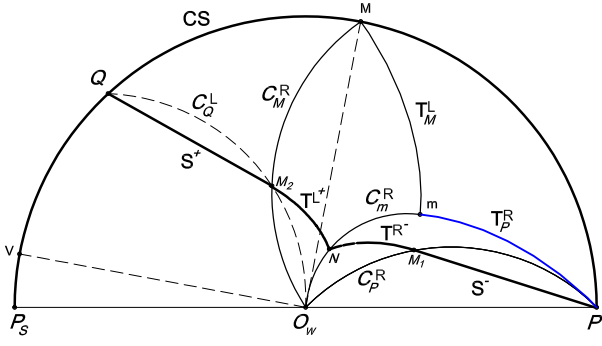


Fig. 9. Optimal path from Q on CS , between M and V , to P . The locus of switching points between extremals S^+ and T^{L+} is the arc of circle C_M^R , whereas the locus of switching points between T^{L+} and T^{R-} is C_m^R .

Proof: From Proposition 6, the switching point M_1 between T^{R-} and S^- belongs to C_P^R .

In the proof of Theorem 4, for $Q \in CS$ with $\psi_M < \psi_Q < \psi_V$, the relation $\psi_Q = 2\alpha_{M_1} + \psi_M$ between angles in the optimal path has been obtained. Hence, from (14), (16), and (17), the coordinates of the switching points N are given by

$$\rho_N = \rho_{M_1} e^{(-\frac{\psi_M}{2})t} = \rho_{M_1} \sin^2 \phi \quad (24)$$

and

$$\psi_N = \alpha_{M_1} + \frac{\psi_M}{2}. \quad (25)$$

Hence, N corresponds to M_1 after a rotation of $\frac{\psi_M}{2}$ and a scaling by $e^{(-\frac{\psi_M}{2})t} = \sin^2 \phi$, which do not depend on ψ_Q . Notice that, applying the same rotation and scaling, $P = (\rho_P, 0)$ is transformed in m , and the right ϕ -arc C_P^R goes in C_m^R . Hence, the locus of switching points N is C_m^R .

Finally, for the palindromic symmetry of optimal paths, it holds that $\rho_{M_1} = \rho_{M_2}$, $\alpha_{M_1} = \alpha_{M_2}$ and $\psi_Q - \alpha_{M_2} = \alpha_{M_1} + \psi_M$. Hence, M_2 corresponds to M_1 after a rotation ψ_M , which does not depend on Q . With the same rotation, P is transformed in M and the locus of switching points M_1 , C_P^R , in the locus of switching points M_2 , C_M^R . ■

Finally, for $Q \in CS$ with $\psi_V \leq \psi_Q < \pi$, the switching locus reduces to the origin O_w . We provide an explicit procedure to compute the switching points for any given $Q \in CS$:

Proposition 14. Given $Q = (\rho_Q, \psi_Q) \in CS$,

- for $0 < \psi_Q \leq \psi_M$, the switching point is $T_P^R \cap T_Q^L$;
- for $\psi_M < \psi_Q < \psi_V$, the switching points are $M_2 \in C_M^R \cap C_Q^L$, $N \in C_m^R \cap T_{M_2}^L$, and $M_1 \in C_P^R \cap T_N^R$.
- for $\psi_V \leq \psi_Q < \pi$, the switching point is O_w .

Proof: From the proof of Proposition 12, for $Q \in CS$ with $0 < \psi_Q \leq \psi_M$, the switching point is $T_Q^L \cap T_P^R = (\rho_P e^{-\frac{\psi_Q}{2}t}, \frac{\psi_Q}{2})$.

From Proposition 13 and Proposition 6, for a given $Q \in CS$ with $\psi_M < \psi_Q < \psi_V$, the switching point M_2 of the optimal path from Q to P is the intersection point between C_M^R and C_Q^L that is univocally determined.

N belongs to C_m^R and lays on the arc T^L . Hence, it can be computed from M_2 as $C_m^R \cap T_{M_2}^L$.

M_1 belongs to C_P^R and lays on the arc T^R . Hence, it can be computed from N as $C_P^R \cap T_N^R$.

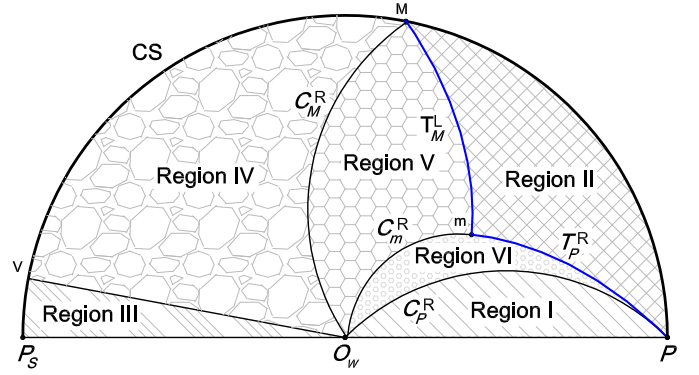


Fig. 10. Partition of DS .

Finally, for $\psi_V \leq \psi_Q < \pi$, the optimal path is characterized by $\alpha_{M_1} = \phi$ (proof of Theorem 4). From (14) and (16) it holds $\rho_N = \rho_{M_1} = \rho_{M_2} = 0$. Hence, in this case, the switching point is O_w . ■

V. OPTIMAL PATHS FOR POINTS IN THE HALF-DISC DS

Having solved the optimal synthesis for points on the boundary of DS , we now address optimal paths for internal points in DS by using the following simple idea: for any $Q \in DS \setminus \partial DS$, find a point $S \in \partial DS$ such that an optimal path γ from S to P goes through Q . By Bellman's optimality principle, the sub-path from Q to P is also optimal.

Consider the partition of DS in six regions illustrated in fig. 10.

Regions of the partition are generalized polygons whose vertices are the characteristic points in DS and whose boundaries belong either to the extremal curves, to the switching loci, or to ∂DS (cf. section IV). All regions have three vertices, except Region I which has two. The boundary arc T_P^R between Region II and Region VI is a degenerate case of measure zero in DS , and will be denoted as Region II'.

Theorem 5. The optimal synthesis for $Q \in DS$ is described in fig. 10 and table I. For each region, the associated optimal path type entirely defines a feasible path of minimum length to the goal.

Region	Included Vertices	Included Boundaries	Optimal Path Type
I	O_w	$C_P^R, O_w P$	S^-
II	M	CS, T_M^L	$T^{L+} * T_P^{R-}$
II'	m	T_P^R	T_P^{R-}
III	V	$P_s O_w, O_w V, CS$	$S^+ * S^-$
IV		CS	$S^+ T^{L+} * T^{R-} S^-$
V		C_M^R	$T^{L+} * T^{R-} S^-$
VI		C_m^R	$T^{R-} S^-$

TABLE I
OPTIMAL SYNTHESIS IN THE HALF-DISC DS .

Proof: We study each region separately:

Region I: From any point in this region it is possible to reach P with a straight path (in backward motion) without violating the FOV constraints (cf. Proposition 5). Such path is obviously optimal.

Region II: For any Q in Region II consider the point s obtained by intersecting the spiral T_Q^L with CS . By the non-intersecting properties of left spirals, s lies between P and M on CS . By Theorem 4 the optimal path γ_s from s to P is of type $T_s^{L+} * T_P^{R-}$. The path $T_Q^{L+} * T_P^{R-}$ from Q is a sub-path of γ_s , hence it is also optimal.

Region II': For any Q in the arc of T_P^R from m to P , the path T_P^{R-} from Q to P is a degenerate case of $T^{L+} * T_P^{R-}$ with a zero-length T^{L+} arc, hence it is also optimal.

Region III: For any Q in Region III consider the line through O_W and Q , which intersects CS in a point s between V and P_s . By Theorem 4, the optimal path from s to P is of type $S^+ * S^-$ with the switch $*$ in O_W , hence (by the same argument) the thesis.

Region IV: For any Q in Region IV consider the left ϕ -arc C_Q^L , and the intersection point $r = C_Q^L \cap C_M^R \setminus O_W$.

Consider now the straight line through Q and r , and let its intersection with CS be denoted s . Such intersection lies between V and M . Indeed, the arc of circle through s , r and O_W is C_V^L and V is such that C_V^L is tangent to C_M^R in O_W . Hence, by Theorem 4, the optimal path γ_s is of type $S^+ T^{L+} * T^R S^-$. By Remark (4), γ_s contains Q in its first straight line segment, hence the thesis.

To finalize the synthesis, we recall that, as a straightforward consequence of Proposition 13, the optimal path for $Q \in C_M^R$ is of type $T_Q^{R-} S^-$, while for $Q \in C_M^R$, the optimal path type is $T_Q^{L+} * T^R S^-$, where the two spiral extremals have the same length. Hence we have:

Region V: For any Q in Region V consider the intersection point s of the spiral T_Q^L with C_M^R . The optimal path γ_s from $s \in C_M^R$ to P is of type $T_s^{L+} * T^R S^-$, and contains Q in its first arc, hence the thesis.

Region VI: For any Q in Region VI consider the intersection point s of the spiral T_Q^R with C_m^R . The optimal path γ_s from $s \in C_m^R$ to P is of type $T_s^{R-} S^-$ and contains Q in its first arc, hence the thesis. ■

Remark 7. From the argument of the proof above and Proposition 3, the existence of optimal paths from points in DS follows directly.

VI. OPTIMAL PATHS FOR POINTS OUTSIDE DS

In this section we exploit the properties of the path transform F_Q to extend the optimal synthesis outside the half-disk DS .

Indeed, recall from section III that F_Q transforms a path from Q to P in a path from $f_Q(P) = \left(\frac{\rho_P^2}{\rho_Q}, \psi_Q\right)$ to P . To highlight the dependence of the new initial point $f_Q(P)$ on Q , we will use alternatively the notation $F(Q) := f_Q(P)$. Notice that $F : \mathbb{R}^2 \setminus (0, 0) \rightarrow \mathbb{R}^2$ is continuous and is an involution, i.e. $F(F(Q)) \equiv Q$, hence $F^{-1} = F$. The locus of fixed points of F is CS . Notice also that, if Q is inside the half-disk DS , $F(Q)$ is outside, and viceversa.

To relate regions of the optimal synthesis inside and outside DS we need the following definition.

Definition 7. Two regions A and B are complementary ($A \rightsquigarrow B$) when $Q \in A \Leftrightarrow F(Q) \in B$.

It is worthwhile to highlight the following result, which is an immediate consequence of Proposition 1:

Proposition 15. If $A \rightsquigarrow B$, optimal paths from points $Q \in A$ of type w_A are mapped by F_Q in optimal paths from $F(Q) = f_Q(P) \in B$ of type $w_B = F_Q(w_A)$.

Remark 8. Existence of optimal paths from points in the upper half-plane outside DS follows from Remark 7 and the previous proposition. Indeed, for any point $Q \notin DS$, an optimal path from $F(Q) \in DS$ to P exists, which is mapped by F_Q in an optimal path from Q to P . Piecing together this with the results of Proposition 3 and Remark 7, and using the symmetry of optimal paths in the lower half-plane, we thus have established the global existence of optimal paths to our problem.

To determine the borders of the regions outside DS we now describe how F maps the borders of regions inside DS .

Proposition 16. Map F transforms:

- 1) arcs of CS into themselves;
- 2) line segments from $Q \in DS$ to O_W in half-lines from $F(Q)$ to infinity with the same slope;
- 3) arcs of a right spiral T_Q^R in arcs of a left spiral $T_{F(Q)}^L$, and viceversa;
- 4) arcs of a circle C_Q^R with $Q \in DS$ in half-lines from $F(Q)$ with slope $\tan(\phi + \psi_Q)$

Proof:

- 1) The first statement follows straightforwardly from the definition of points of CS .
- 2) Points on the segment from O_W to $Q \in DS$ have polar coordinates (ρ, ψ_Q) with $\rho \in (0, \rho_Q]$. Such points are mapped by F in $(\rho_P^2/\rho, \psi_Q)$ with $\rho_P^2/\rho \in [\rho_P^2/\rho_Q, +\infty)$, hence in the half-line from $F(Q) = (\rho_P^2/\rho_Q, \psi_Q)$ with slope ψ_Q .
- 3) Points on the arc of a right spiral T^R from $A = (\rho_A, \psi_A)$ to $B = (\rho_A e^{(\psi_A - \psi_B)t}, \psi_B)$ have coordinates $(\rho_A e^{(\psi_A - \psi)t}, \psi)$ with $\psi \in [\psi_A, \psi_B]$. Map F transforms such points in $(\rho_P^2/\rho_A e^{-(\psi_A - \psi)t}, \psi)$. These are points on a left spiral T^L from $F(A) = (\rho_P^2/\rho_A, \psi_A)$ to $F(B) = (\rho_P^2/\rho_A e^{-(\psi_A - \psi_B)t}, \psi_B)$. The viceversa follows from the involutive property of F .
- 4) Points of C_Q^R have coordinates $(\rho_Q \sin(\phi - \psi + \psi_Q)/\sin \phi, \psi)$ with $\psi \in [\psi_Q, \psi_Q + \phi]$. Such points are mapped in $(\rho_P^2 \sin \phi / (\rho_Q \sin(\phi - \psi + \psi_Q)), \psi)$. On the other hand, the straight line from $F(Q)$ forming an angle $\phi + \psi_Q$ with the X_W axis is described by the equation

$$y = \tan(\phi + \psi_Q)x - \frac{\rho_P^2}{\rho_Q} \frac{\sin \phi}{\cos(\phi + \psi_Q)}.$$

Rewriting this equation in polar coordinates, it is straightforward to check that it is satisfied by the image of C_Q^R under F , hence the thesis. ■

Let r_P be the right ϕ -radius in P of equation $y = \tan \phi(x - \rho_P)$; X_W^+ (X_W^-) the half-line from P (P_S) in the direction of the positive (negative) X_W axis; r_V the half-line from V parallel to $\overline{O_W V}$; r_M the right ϕ -radius in M , which is tangent to the spiral T_M^L , and r_{M_m} the right ϕ -radius in

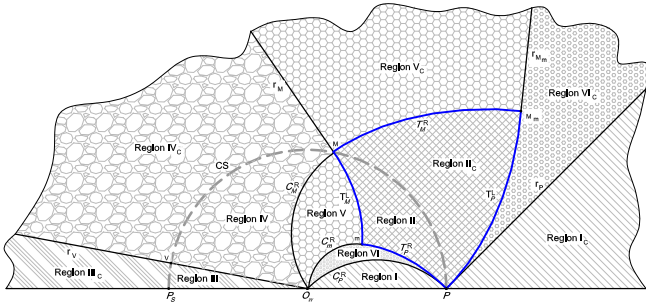


Fig. 11. Partition of the upper half-plane with $\phi = \pi/4$.

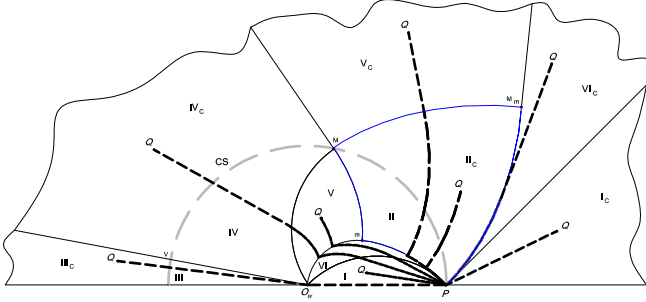


Fig. 12. Examples of optimal paths from points Q in different regions to P .

$M_m = F(m)$ which is tangent to the spiral T_P^L . Notice that r_{M_m} is described by the equation

$$y = \tan\left(\phi + \frac{\psi_M}{2}\right) \left(x - \frac{\rho_P}{\sin \phi \sin\left(\phi + \frac{\psi_M}{2}\right)}\right).$$

Theorem 6. *The optimal synthesis for Q outside DS is described in fig. 11 and table II.*

Region	Included Vertices	Included Boundaries	Optimal Path Type
I _c		X_W^+, r_P	S^+
II _c		T_M^R	$T^{L+} * T_P^{R-}$
II' _c	M_m	T_P^L	T_P^{L+}
III _c		r_V, X_W^-	$S^+ * S^-$
IV _c			$S^+ T^{L+} * T^{R-} S^-$
V _c		r_M	$S^+ T^{L+} * T_P^{R-}$
VI _c		r_{M_m}	$S^+ T_P^{L+}$

TABLE II
OPTIMAL SYNTHESIS OUTSIDE THE HALF-DISC DS .

Proof: We only need to show that Region “R” and Region “R_c” are complementary, for $R = I, II, \dots VI$. To do so, by continuity of F , it will be enough to prove that the borders of R are mapped in the borders of R_c. This is in turn a direct consequence of application of Proposition 16. ■

VII. GLOBAL OPTIMAL SYNTHESIS

From results in section V and VI, it can be observed that optimal paths from Region II and II_c are of the same type, i.e. $w_{II} = w_{II_c}$. The same holds for Region III and III_c, and for Region IV and IV_c. These three pairs of regions can be merged in a single region in the final partition of the plane.

The optimal path synthesis can be therefore summarized as reported in fig. 11 and in table III. Conditions on ρ_Q and ψ_Q determining the inclusion of Q in each Region are also reported in table III in term of a number of elementary inequalities.

```

1: procedure REGIONTEST( $\rho_Q, \psi_Q$ )
2:   Constant Parameters:  $\phi, \rho_P$ 
3:   if  $\psi_Q \leq \psi_m$  then
4:     if  $\rho_Q \leq \rho_P \frac{\sin(\phi - \psi_Q)}{\sin \phi}$  then { $Q$  is below or on  $C_P^R$ }
5:       return Region I
6:     else if  $\rho_Q < \rho_P e^{-\psi_Q}$  then { $Q$  is below  $T_P^R$ }
7:       return Region VI
8:     else if  $\rho_Q = \rho_P e^{-\psi_Q}$  then { $Q$  is on  $T_P^R$ }
9:       return Region II'
10:    else
11:      return Region II
12:    end if
13:  else if  $\psi_Q \leq \psi_M$  then
14:    if  $\rho_Q \leq \rho_P \sin \phi \sin(\phi - \psi_Q)$  &&  $\psi_Q \leq \psi_m + \phi$  then { $Q$  is below
or on  $C_m^R$ }
15:      return Region VI
16:    else if  $\rho_Q \leq \rho_P e^{(\psi_Q - \psi_M)}$  then { $Q$  is below or on  $T_M^L$ }
17:      return Region V
18:    else
19:      return Region II
20:    end if
21:  else if  $\psi_Q \leq \psi_V$  then
22:    if  $\rho_Q \leq \rho_P \frac{\sin(\phi - \psi_Q)}{\sin \phi}$  &&  $\psi_Q \leq \psi_m + \phi$  then { $Q$  is below or on
 $C_M^R$ }
23:      return Region V
24:    else
25:      return Region IV
26:    end if
27:  else
28:    return Region III
29:  end if
30: end procedure

```

Fig. 13. Region Test Algorithm for points inside CS

Given any initial position Q inside CS , algorithm reported in fig. 13 returns the Region in which Q lays. For an external point Q ($\rho_Q > \rho_P$), the procedure is applied to $F(Q)$, i.e. replacing ρ_Q with $\frac{\rho_P^2}{\rho_Q}$ and complementing the output region.

Remark 9. *The region in which $Q = (\rho_Q, \psi_Q)$ lays can be determined verifying at most 6 inequalities on ρ_Q and ψ_Q . Indeed, the first inequality is the test $\rho_Q \geq \rho_P$, while algorithm reported in fig. 13 consists in at most 5 inequality tests.*

Examples of optimal paths from points of different regions are plotted in fig. 12.

It should be noticed that, while the obtained synthesis is valid in general, the position of the characteristic points and the shape of the regions varies with the FOV angle ϕ : compare e.g. the partition in fig. 11, obtained for $\phi = \pi/4$, with the partition corresponding to $\phi = \pi/3$, which is reported in fig. 14.

A particular case occurs for $\phi = \pi/2$ (see fig. 15). Here, $M \equiv m \equiv M_m \equiv P$, $C_m^R \equiv C_M^R \equiv C_P^R$, and the spiral arcs T_P^R and T_P^L degenerate to zero length in a point on C_P^R . All optimal paths turn out to be of type $S^+ * S^-$, S^+ , or S^- .

The partition of the whole plane of motion is obtained simply by symmetry with respect to the X_W axis, and is reported for completeness in fig. 16. Regions in the lower half-plane are denoted with a subscript s (for symmetry), and are associated to optimal words obtained exchanging superscript R with L in the words reported in table III for the symmetric region.

A comparison with the synthesis obtained in [13], reported in fig. 17, is in order at this point. As it can be easily

Region	Optimal Path Type	Inclusion Conditions
I	S^-	$\rho_Q \leq \rho_P \frac{\sin(\phi - \psi_Q)}{\sin \phi}$, $\psi_Q \leq \phi$
I _c	S^+	$\rho_Q \geq \rho_P \frac{\sin \phi}{\sin(\phi - \psi_Q)}$, $\psi_Q \leq \phi$
II ∪ II _c	$T^{L+} * T_P^{R-}$	$\rho_P e^{(\psi_Q - \psi_M)t} \leq \rho_Q \leq \rho_P e^{-(\psi_Q - \psi_M)t}$, $\rho_P e^{-\psi_Q t} < \rho_Q < \rho_P e^{\psi_Q t}$, $\psi_Q \leq \psi_M$
II'	T_P^{R-}	$\rho_Q = \rho_P e^{-\psi_Q t}$, $\psi_Q \leq \frac{\psi_M}{2}$
II' _c	T_P^{L+}	$\rho_Q = \rho_P e^{\psi_Q t}$, $\psi_Q \leq \frac{\psi_M}{2}$
III ∪ III _c	$S^+ * S^-$	$2\phi + \psi_M \leq \psi_Q \leq \pi$
IV ∪ IV _c	$S^+ T^{L+} * T^R S^-$	$\rho_P \frac{\sin(\phi - \psi_Q)}{\sin \phi} \leq \rho_Q \leq \rho_P \frac{\sin \phi}{\sin(\phi - \psi_Q)}$, $\psi_M \leq \psi_Q \leq 2\phi + \psi_M$
V	$T^{L+} * T^R S^-$	$\rho_Q \leq \rho_P \frac{\sin \phi}{\sin(\phi - \psi_Q)}$, $\rho_P e^{-(\psi_Q - \psi_M)t} \leq \rho_Q \leq \rho_P e^{(\psi_Q - \psi_M)t}$, $\frac{\psi_M}{2} \leq \psi_Q \leq \psi_M + \phi$
V _c	$S^+ T^{L+} * T_P^{R-}$	$\rho_P \frac{\sin \phi}{\sin(\phi - \psi_Q)} \leq \rho_Q \leq \rho_P \frac{1}{\sin \phi \sin(\phi - \psi_Q)}$, $\rho_Q \geq \rho_P e^{-(\psi_Q - \psi_M)t}$, $\frac{\psi_M}{2} \leq \psi_Q \leq \psi_M + \phi$
VI	$T^R S^-$	$\rho_P \frac{\sin(\phi - \psi_Q)}{\sin \phi} \leq \rho_Q \leq \rho_P \sin \phi \sin(\phi - \psi_Q)$, $\rho_Q \leq \rho_P e^{-\psi_Q t}$, $\psi_Q \leq \phi + \frac{\psi_M}{2}$
VI _c	$S^+ T_P^{L+}$	$\rho_P \frac{1}{\sin \phi \sin(\phi - \psi_Q)} \leq \rho_Q \leq \rho_P \frac{\sin \phi}{\sin(\phi - \psi_Q)}$, $\rho_Q \geq \rho_P e^{\psi_Q t}$, $\psi_Q \leq \phi + \frac{\psi_M}{2}$

TABLE III
OPTIMAL SYNTHESIS IN THE UPPER HALF-PLANE AND REGION
INCLUSION CONDITIONS FOR INITIAL POSITION Q .

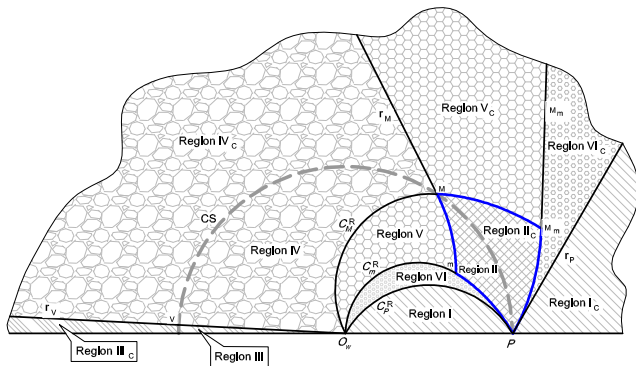


Fig. 14. Partition of the upper half plane with $\phi = \pi/3$.

checked, the synthesis in [13] is correct for all initial points that are inside a circle centered in the goal point P and going through the characteristic point m . However, extrapolation of the synthesis in [13] outside this circle leads to quite different results from our synthesis, which is valid globally.

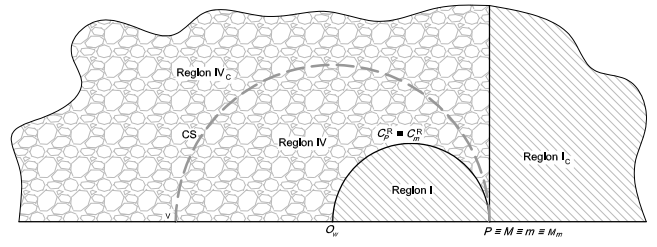


Fig. 15. Partition of the upper half plane with $\phi = \pi/2$.

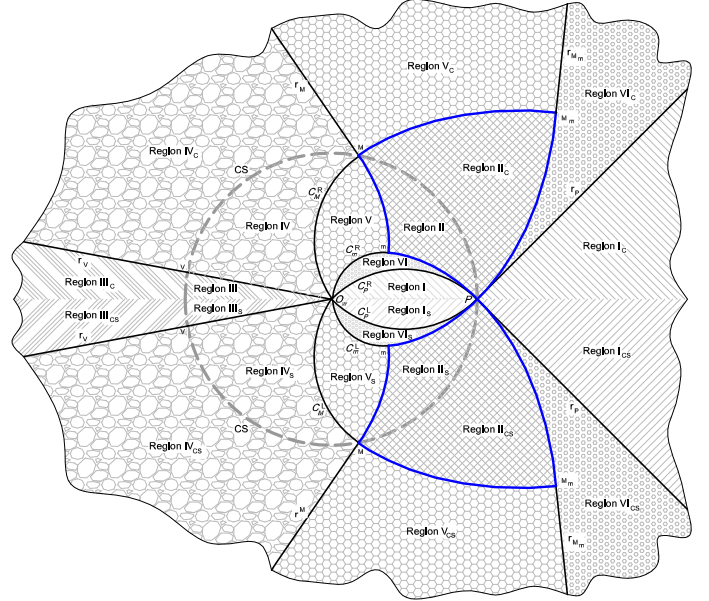


Fig. 16. Partition of the (X_W, Z_W) plane with $\phi = \pi/4$.

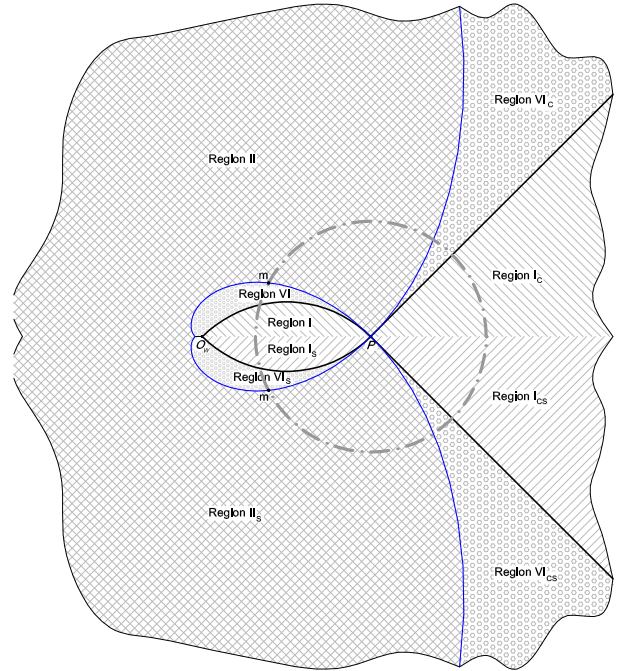


Fig. 17. Partition of the (X_W, Z_W) plane with $\phi = \pi/4$ according to [13].

VIII. CONCLUSIONS AND FUTURE WORK

We have provided a complete characterization of shortest paths for a moving directed point with nonholonomic kine-

matics to reach a target while keeping a fixed point within a conical region relative to itself. Symmetries and invariants of the problem have been exploited to determine optimal paths from any point of the motion plane to the goal, providing a substantial refinement and correction of existing results. Applications of these results to robotics will enable for instance to plan shortest paths for a wheeled platform with unicycle-like kinematics so that a given feature is maintained inside the limited field-of-view of a camera mounted on board. Indeed, the robot can use the provided algorithm to determine the region where it stands based on the current position verifying at most 6 inequalities.

Several extensions of the considered problem are possible and are the objectives of current work. In the present setup, we have ignored constraints on the vertical position of the feature in the image plane. While this is perfectly acceptable for features that lie in the motion plane, a further vertical constraint on the FOV should be considered in general, which would induce an off-limit zone for the robot close to the feature position. Furthermore, the problem of determining optimal paths in the case of more than one feature would also be useful to consider. Finally, different cost functions to be minimized can be considered, such as e.g. the time to reach the goal, and different types of vehicles (e.g. Dubins' or Reeds and Shepp's cars of limited curvature).

REFERENCES

- [1] V. A. Tucker, "The deep fovea, sideways vision and spiral flight paths in raptors," *The Journal of Experimental Biology*, pp. 3745–3754, 2000.
- [2] L. E. Dubins, "On curves of minimal length with a constraint on average curvature, and with prescribed initial and terminal positions and tangents," *American Journal of Mathematics*, pp. 457–516, 1957.
- [3] X. Bui, P. Souères, J.-D. Boissonnat, and J.-P. Laumond, "Shortest path synthesis for Dubins non-holonomic robots," in *IEEE International Conference on Robotics and Automation*, 1994, pp. 2–7.
- [4] J. A. Reeds and L. A. Shepp, "Optimal paths for a car that goes both forwards and backwards," *Pacific Journal of Mathematics*, pp. 367–393, 1990.
- [5] H. Sussmann and G. Tang, "Shortest paths for the reeds-shepp car: A worked out example of the use of geometric techniques in nonlinear optimal control," Rutgers Cent. Syst. Control Tech. Rep. 91-10, Sep. 1991.
- [6] H. Souères and J. P. Laumond, "Shortest paths synthesis for a car-like robot," *IEEE Transaction on Automatic Control*, pp. 672–688, 1996.
- [7] H. Chitsaz, S. M. LaValle, D. J. Balkcom, and M. Mason, "Minimum wheel-rotation for differential-drive mobile robots," *The International Journal of Robotics Research*, pp. 66–80, 2009.
- [8] H. Wang, Y. Chan, and P. Souères, "A geometric algorithm to compute time-optimal trajectories for a bidirectional steered robot," *IEEE Transaction on Robotics*, pp. –, 2009.
- [9] D. Balkcom and M. Mason, "Time-optimal trajectories for an omnidirectional vehicle," *The International Journal of Robotics Research*, vol. 25, no. 10, pp. 985–999, 2006.
- [10] G. Chesi and Y. Hung, "Global path-planning for constrained and optimal visual servoing," *IEEE Transactions on Robotics*, vol. 23, no. 5, pp. 1050–1060, October 2007.
- [11] K. Deguchi, "Optimal motion control for image-based visual servoing by decoupling translation and rotation," in *IEEE/RJS Intl. Conf. on Intelligent Robots and Systems*, Victoria, B.C., Canada, October 1998, pp. 705–711.
- [12] Y. Mezouar, A. Remazeilles, P. Gros, and F. Chaumette, "Images interpolation for image-based control under large displacement," in *Proc. IEEE Int. Conf. on Robotics and Automation*, Washington, DC, May 2002, pp. 3787–3794.
- [13] S. Bhattacharya, R. Murrieta-Cid, and S. Hutchinson, "Optimal paths for landmark-based navigation by differential-drive vehicles with field-of-view constraints," *IEEE Transactions on Robotics*, vol. 23, no. 1, pp. 47–59, February 2007.
- [14] P. Salaris, F. A. W. Belo, D. Fontanelli, L. Greco, and A. Bicchi, "Optimal paths in a constrained image plane for purely image-based parking," *IROS*, pp. 1673–1680, 2008.
- [15] A. Bryson and Y. Ho, *Applied optimal control*. Wiley New York, 1975.
- [16] L. Cesari, *Optimization-theory and applications: problems with ordinary differential equations*. Springer-Verlag, New York, 1983.



Paolo Salaris Paolo Salaris received the "Laurea" degree in Electrical Engineering from the University of Pisa in 2007. Currently, he is a PhD student in Robotics, Automation and Bioengineering at the University of Pisa. He has been Visiting Scholar at the Beckman Institute for advanced science and technology in the Artificial intelligence group, University of Illinois at Urbana-Champaign. His main research interests within Robotics are in optimal motion planning, control for nonholonomic vehicles and visual servo control.



Daniele Fotanelli received the M.S. degree in Information Engineering in 2001, and the Ph.D. degree in Automation, Robotics and Bioengineering in 2006, both from the University of Pisa, Pisa, Italy. He was a Visiting Scientist with the Vision Lab of the University of California at Los Angeles, Los Angeles, US, from 2006 to 2007. From 2007 to 2008, he has been an Associate Researcher with the Interdepartment Research Center "E. Piaggio", University of Pisa. From 2008 he joined as an Associate Researcher the Department of Information Engineering and Computer Science, University of Trento, Trento, Italy. His research interests include robotics and visual servoing, embedded system control, wireless sensor networks, networked and distributed control.



Lucia Pallottino received the "Laurea" degree in Mathematics from the University of Pisa in 1996, and the Ph.D. degree in Robotics and Industrial Automation degree from the University of Pisa in 2002. She has been Visiting Scholar in the Laboratory for Information and Decision Systems at MIT, Cambridge, MA and Visiting Researcher in the Mechanical and Aerospace Engineering Department at UCLA, Los Angeles, CA. She joined the Faculty of Engineering in the University of Pisa as an Assistant Professor in 2007. Her main research interests within Robotics are in optimal motion planning and control for nonholonomic vehicles, multi-agent systems and cooperating objects, optimal control, and Air Traffic Management Systems.



Antonio Bicchi is Professor of System Theory and Robotics at the University of Pisa. He graduated at the University of Bologna in 1988 and was a postdoc scholar at M.I.T. A.I. Lab in 1988–1990. His main research interests are in Dynamics, kinematics and control of complex mechanical systems, including robots, autonomous vehicles, and automotive systems; Haptics and dextrous manipulation; Theory and control of nonlinear systems, in particular hybrid (logic/dynamic, symbol/signal) systems. He has published more than 200 papers on international journals, books, and refereed conferences. He currently serves as the Director of the Interdepartmental Research Center "E. Piaggio" of the University of Pisa, and as Editor in Chief of the Conference Editorial Board for the IEEE Robotics and Automation Society (RAS). Antonio Bicchi is an IEEE Fellow since 2005. He has served as Vice President of IEEE RAS, Distinguished Lecturer, and editor for several scientific journals including Transactions on Robotics and Automation and Int.J. Robotics Research. He has organized and co-chaired the first WorldHaptics Conference (2005) and Hybrid Systems: Computation and Control (2007).